

## Comparisons of the genome of SARS-CoV-2 and those of other betacoronaviruses

Eduardo Rodríguez-Román<sup>1\*</sup> and Adrian J. Gibbs<sup>2</sup>

1. *Center for Microbiology and Cell Biology, Instituto Venezolano de Investigaciones Científicas, Caracas 1020A, Venezuela*
2. *Emeritus Faculty, Australian National University, Canberra, ACT 2601, Australia*

**Corresponding author:** Eduardo Rodríguez-Román, PhD

Center for Microbiology and Cell Biology, Instituto Venezolano de Investigaciones Científicas (IVIC). Carretera Panamericana, Km 11. P.O. Box 20632. Caracas 1020A, Venezuela; Tel: +58(212)504-1189; Fax: +58(212)504-1500; Email: [erodriguezroman@gmail.com](mailto:erodriguezroman@gmail.com)

### Abstract

The genome of SARS-CoV-2 virus causing the worldwide pandemic of COVID-19 is most closely related to viral metagenomes isolated from bats and, more distantly, pangolins. All are of sarbecoviruses of the genus *Betacoronavirus*. We have unravelled their recombinational and mutational histories. All showed clear evidence of recombination, most events involving the 3' half of the genomes. The 5' region of their genomes was mostly recombinant free, and a phylogeny calculated from this region confirmed that SARS-CoV-2 is closer to RmYN02 than RaTG13, and showed that SARS-CoV-2 diverged from RmYN02 at least 26 years ago, and both diverged from RaTG13 at least 37 years ago; recombinant regions specific to these three viruses provided no additional information as they matched no other Genbank sequences closely. Simple pairwise comparisons of genomes show that there are three regions where most non-synonymous changes probably occurred; the DUF3655 region of the nsp3, the S gene and ORF 8 gene. Differences in the last two of those regions have probably resulted from recombinational changes, however differences in the DUF3655 region may have resulted from selection. A hexamer of the proteins encoded by the nsp3 region may form the molecular pore spanning the double membrane of the coronavirus replication organelle (Wolff et al., 2020), and perhaps the acidic polypeptide encoded by DUF3655 lines it, and presents a novel target for pharmaceutical intervention.

**Keywords:** betacoronaviruses, phylogeny, evolution, SARS-CoV-2, DUF3655, pharmaceutical intervention.

## 1 **1. Introduction**

2 The family *Coronaviridae* is divided into two subfamilies, five genera, 26 subgenera, and 46  
3 species (International Committee on Taxonomy of Viruses; <https://talk.ictvonline.org/>). However,  
4 only members of the genera *Alphacoronavirus* and *Betacoronavirus* have been reported to infect  
5 humans. Coronaviruses (CoVs) have single-stranded positive-sense RNA genomes that are  
6 several-fold larger than those of other RNA viruses (Anthony et al., 2017); this reflects the fact  
7 that the CoV nsp14 is a proof-reading bi-functional enzyme, ExoN (Ferron et al., 2018) responsible  
8 for recombination (Gribble et al., 2020).

9 In December of 2019 a novel coronavirus causing pneumonia emerged in Wuhan, China  
10 (Wu et al., 2020). Initially, the virus was called 2019-nCoV, but it is now known as SARS-CoV-  
11 2 (Gorbalenya et al., 2020), and is the etiologic agent of the disease COVID-19. It is the seventh  
12 CoV of humans to be reported (Rodríguez-Román and Gibbs, 2020; Ye et al., 2020), and it has  
13 generated a pandemic with more than 10 million people infected, and 0.5 million people dead by  
14 the end of June 2020. While trying to establish from where this virus emerged, there have been  
15 conflicting claims that it may have come from bats or pangolins, and is most closely related to  
16 either the YN02 virus or the RaTG13 virus (Li et al., 2020; Lin and Chen, 2020; Wang et al., 2020;  
17 Xiao et al, 2020; Zhou et al., 2020), and in this short paper we resolve some of these differences  
18 and discuss an interesting betacoronavirus region - DUF3655!

19

20

## 21 **Methods**

22 Sequences were downloaded from the Genbank and GISAID databases. They were edited  
23 using BioEdit (Hall, 1999), aligned using the neighbor-joining (NJ) option of ClustalX  
24 (Jeanmougin et al., 1998), and the maximum likelihood (ML) method PhyML 3.0 (ML) (Guindon  
25 and Gascuel, 2003). Sequences were tested for the presence of phylogenetic anomalies using the  
26 full suite of options in RDP4 with default parameters (Maynard-Smith, 1992; Holmes et al., 1999;  
27 Padidam et al., 1999; Gibbs et al., 2000; Martin and Rybicki, 2000; McGuire and Wright, 2000;  
28 Posada and Crandall, 2001; Martin et al., 2005; Boni et al., 2007; Lemey et al., 2009; Martin et  
29 al., 2015); anomalies found by four or fewer methods and with greater than  $10^{-5}$  random probability  
30 were ignored; statistical support for their topologies was assessed using the SH method  
31 (Shimodaira and Hasegawa, 1999). Trees were drawn using Figtree Version 1.3  
32 (<http://tree.bio.ed.ac.uk/software/figtree/>; 12 May 2018) and a commercial graphics package.  
33 Patristic distances within trees were calculated using Patristic 1.0 (Fourment and Gibbs, 2006) to  
34 convert trefiles to matrices of pairwise branch lengths.

35 Pairs of sequences were individually aligned using the TranslatorX server (Abascal et al.,  
36 2010; <http://translatorx.co.uk>). They were then compared using the DnDscan method (Gibbs et  
37 al., 2007), which is a simple heuristic method for scanning aligned sequences, codon-by-codon

38 and codon position-by-position, to identify the NS and S changes that may have occurred  
39 converting one codon to the other. NS and S variation is taken to be the sum of the scores for all  
40 pairwise position comparisons within that codon. Each comparison involves substituting a  
41 nucleotide of one codon with the homologous nucleotide of the other codon and then checking  
42 how this affects the amino acid it encodes using the standard genetic code. The process is then  
43 reversed, replacing the nucleotides of the second codon of the pair with those of the first, again  
44 only one at a time. Thus, there are six possible exchanges between a single codon pair. If, say, the  
45 first codon is ACT (Thr) and the second GGA (Gly), then all three nucleotides differ and six out  
46 of six changed codons are produced. Substituting of the first position of ACT (Thr) with the first  
47 nucleotide of the second codon (GGA) will generate GCT (Ala), a NS change, and similarly  
48 substituting of the second position C with the second position G generates AGT (Ser), also a NS  
49 change, and the third generates ACA (Thr), a S change. Likewise swapping the second GGA  
50 (Gly) generates AGA (Arg), GCA (Ala) and GGT (Gly), which are NS, NS and S changes  
51 respectively. In all, the pairwise comparison provides a score of 2/6 S changes, and 4/6 to the NS.  
52 Pairs of codons that are identical merely contribute 0/6 to both the total S and NS scores for the  
53 window position, and indels are treated as 6/6 NS changes. These calculations make no assumption  
54 about the direction of evolutionary change nor of the optimal or most parsimonious path of  
55 substitution between two codons. The aim is to assess each of the single possible substitutions  
56 indicated by two homologous but different codons. The results for each codon position in the  
57 alignment are recorded in a CSV file so that they can be further processed for viewing. The scores  
58 used for Fig. 3, for example, were running (overlapping) sums of 5 codon scores, and thus the  
59 NS=5.0 maxima represent five adjacent codons each with a maximum NS score of one.

60 The theoretical isoelectric points of the DUF3655 peptides were calculated using the online  
61 ProtParam facility of the ExPASy (Gasteiger et al., 2005; <https://web.expasy.org/protoparam/>).

62

## 63 **Results**

64 In mid-May 2020 a BLAST search (Altschul et al., 1990) of the Genbank databases was  
65 made using the SARS-CoV-2 Wuhan-Hu-1 sequence (NC\_045512) as a query, and over 100  
66 related full-length genomic sequences were identified. These were downloaded, and two from the  
67 GISAID database that had been discussed in reports, were added (Rodríguez-Román and Gibbs,  
68 2020).

69 The sequences were aligned using MAFFT with its L option. A Neighbor-Joining (NJ)  
70 phylogeny of these sequences identified eight distinct genomic sequences in the SARS-CoV-2  
71 lineage, together with eleven others in a more distant divergence that included the SARS-CoV  
72 reference sequence (NC\_004718), and with an outgroup of ten other coronavirus genomes. These  
73 were checked for recombination using the Recombination Detection Program (RDP 4.95) (Martin  
74 et al., 2015). Recombinants were detected in, and between, all betacoronaviruses, but not between  
75 them and the outgroup sequences. Eleven were chosen for analysis; all eight from the SARS-CoV-

76 2 lineage and three from the SARS-CoV's; Table 1 lists their Accession Codes, hosts, source isolate  
77 codes, and shortened acronyms, which are used hereafter in this paper and its illustrations.

78 Genes are found in all three reading frames of coronavirus genomes, therefore the 11  
79 sequences were aligned using MAFFT-L, and BioEdit (Hall, 1999) was used to create, for each of  
80 the eleven, a single concatenated alignment of their open reading frames (i.e. all the genes in the  
81 same reading frame). We call these, concats. The concats were aligned, using their encoded amino  
82 acids as guide, by the TranslatorX online server (Abascal et al., 2010; <http://translatorx.co.uk>) with  
83 its MAFFT option (Kato and Standley, 2013), and further refined by hand resulting in a concat  
84 alignment of 29,286 nts.

85 The maximum likelihood (ML) phylogeny of the eleven complete sarbecovirus concats  
86 (Fig. 1A), calculated by the PhyML method, confirmed that they form two lineages diverging from  
87 the midpoint root (circled), one including SARS-1 and the other SARS-2. However, the individual  
88 nodes in the SARS-2 crown group were not fully supported statistically in this phylogeny; only an  
89 average of 0.89 SH support for the terminal three nodes of the SARS-2 lineage. The concat  
90 alignment was therefore checked for recombinants using RDP 4.95, and gave the recombinant map  
91 shown in Fig. 2, which shows that all concats have recombinant regions. Notably SARS-2, YN02  
92 and RaTG13, which we call the crown group of the SARS-2 lineage, all have two identically placed  
93 recombinant regions from the same minor 'parent', Rf4092 (i.e. a SARS-1 lineage bat virus).  
94 Significant recombinant regions specific to each these three viruses in the spike region, and 3' to  
95 it, provided no additional phylogenetic or dating information as they matched no other sequences  
96 in Genbank closely (<84% ID).

97 Concats of the basal branches of the phylogeny, ZC45 and ZXC21, have a large central  
98 recombinant region most closely related to the homologous region of HKU3-8, which is of the  
99 SARS-1 lineage. Further recombinant regions were found in all the sequences, but mostly in their  
100 3' terminal halves and, in summary, only one statistically significant recombinant region (i.e. not  
101 marked in Fig. 2 with a black dot at its 5' end) was found between nts 1 and 11496 of all eleven  
102 concats, and that was in the ZC45 sequence (nts 1443-1768; parent 'unknown') (Fig. 2). Thus,  
103 importantly, the 5' terminal region of all eleven concats, stretching from nts 1 to 11496, was  
104 available to obtain a phylogeny based on point mutations alone, and not confounded by  
105 recombination; the ZC45 recombinant is unlikely to have distorted the phylogeny much as it is  
106 only 2.8% of the 11496 nts.

107 Fig. 1B shows the maximum likelihood (ML) phylogeny calculated from nts 1-11496  
108 region of the 11 concats. All nodes in this phylogeny have full statistical support (i.e. 1.0 SH), and  
109 most of the 'root to tip' distances in the tree were similar, unlike those in Fig. 1A; one effect of  
110 recombination. The topology of the '1-11496' tree was different from that of the tree of complete  
111 concats as the SARS-2 concat now groups with all SARS-2 lineage bat isolates, and the pangolin  
112 isolates are now basal. Closest to the SARS-2 concat is the YN02 concat with the RaTG13 concat  
113 a little further away.

114 The minor 'parent' of the shared recombinant regions in the centre of the SARS-2, YN02  
115 and RaTG13 concat (nts 14372-15124 and nts 16383-17566) is Rf4092 of the SARS-1 lineage.  
116 These recombinant regions were not found in the other bat sequences of the SARS-2 lineage  
117 indicating that they resulted from a recombination event that occurred after the crown group  
118 diverged from the ZXC21 and ZC45 branch, but before RaTG13 diverged. Confusingly however  
119 the second of these recombinant regions was also found in the pangolin G/1/19 concat!

120 The recombination map also shows the complex recombinational history of the spike gene,  
121 the position of which is coloured yellow in the simplified genomic map at the top of Fig. 2. This  
122 is confirmed by the phylogeny of that region (Fig. 1C), which is fully supported statistically except  
123 for the SARS-1, Rf4092 and HKU3-8 cluster (mean 0.91 SH). The spike phylogeny has pangolin  
124 genes immediately basal to the SARS-2 and RaTG13 twig, and the spike region of YN02 gene is  
125 shown to be from the SARS-1 lineage. However, it is essential to realize that, although we know  
126 the hosts from which the isolates were collected, other hosts may have been infected *en route*.

127 The dates of the nodes in the '1-11496' SARS-2 phylogeny (Fig. 1B) can be inferred using  
128 published estimates of the evolutionary rate of the SARS-2 population in the human population,  
129 assuming that the pre- and post- emergence rates are the same (Rodríguez-Román and Gibbs,  
130 2020). Various estimates of the SARS-2 evolutionary rate have been published recently;  $1.126 \times$   
131  $10^{-3}$  (95 % BCI:  $1.03\text{--}1.23 \times 10^{-3}$ ) substitutions per site per year (s/s/y) (Candido et al., 2020),  
132  $1.1 \times 10^{-3}$  s/s/y (95% CI  $7.03 \times 10^{-4}$  and  $1.5 \times 10^{-3}$  s/s/y) (Duchêne et al., 2020),  $9.41 \times 10^{-4}$  s/s/y +/-  
133  $4.99 \times 10^{-5}$  (Pybus et al., 2020) and  $8 \times 10^{-4}$  s/s/y (Resende et al., 2020).

134 The mean of these rate estimates is  $0.99 \times 10^{-3}$  s/s/y, and, assuming that the virus is  
135 evolving at the same rate as the '1-11496' region of its genome, then the mean patristic distances  
136 passing through nodes in Fig. 1B suggest that the SARS-2 and YN02 viruses diverged in 1994  
137 CE (26.03 years before present; ybp), they diverged from RaTG13 in 1983 CE (36.8 ybp), and  
138 from ZXC21 and ZC45 in 1936 CE (83.6 ybp) and from G/1/19 in 1908 CE (111.8 ybp). The  
139 standard deviation of the branch length estimates varied between 0.8% and 2.8%. The most  
140 recent estimates are probably the most accurate because although all mutations contribute to the  
141 'molecular clock', most are quickly lost (Duchêne et al. 2014), and therefore times to the older  
142 dates are overestimated. Nonetheless, it is probable that SARS-2 and YN02 diverged over 20  
143 years ago, and the two recombinant regions characteristic of the SARS-2, YN02 and RaTG13  
144 virus genomes were acquired by their shared progenitor more than 30, but less than 80, years  
145 ago! All these datings are based on a large number of assumptions, and could be earlier as  
146 concluded by Wang et al. (2020).

147 Finally, we compared the concat sequences directly in pairs, not only to identify any  
148 regions that were evolving abnormally, but also to confirm the recombination map patterns shown  
149 in Fig. 2. We used the DnDscan method (Gibbs et al., 2007 - see Methods) as this enables simple  
150 visual comparisons to be made, as well as numerical. Fig. 3 shows the synonymous (S - blue) and  
151 non-synonymous (NS - gold) differences in five of 45 pairwise possible comparisons of eleven



152 concats. It can be seen that S differences occur throughout most of the comparisons, but NS  
153 differences are most obvious in three regions of the genomes. There are slightly fewer S  
154 differences between SARS-2 and YN02 than between SARS-2 and RaTG13 or between YN02 and  
155 RaTG13, and this confirms the phylogenetic tree (Fig. 1B); it shows that SARS-2 is closest to  
156 YN02 as the total DnDscan scores for the '1-11496' regions of SARS-2 v YN02 are S 100.0 NS  
157 27.5, but, for the other combinations, S134.0 NS 30.1 and S131.5 NS37.6, respectively. The  
158 largest NS differences are in the DnDscans of the spike protein gene, especially its RBD region  
159 and an adjacent "-PRRA-" insertion (Andersen et al. 2020). Again, the recombination map results  
160 (Fig. 2) are confirmed by the DnDscan as the spike region of the SARS-2 x RaTG13 comparison,  
161 especially its 5' end, has few NS differences, as they share an 'unknown' recombinant (nts 21257 -  
162 22152).

163 There are also two other regions of the concats consistently showing larger numbers of NS  
164 differences. One is centred on the 'Domain of Unknown Function' (DUF) 3655 region of the nsp3,  
165 a "disordered binding region" (Prates et al. 2020), that is N' terminally adjacent to the ADP-ribose  
166 phosphatase. This region of increased NS differences was found to some extent in all concat  
167 comparisons suggesting that its differences result from evolution/selection, whereas the other, the  
168 ORF 8 region near the 3' end of the genome, was not found in some comparisons, such as SARS-  
169 2 x RaTG13, and may therefore have resulted from recombination. The DUF3655 region is  
170 discussed below.

171

## 172 2. Discussion

173 We have discombobulated the recombinational and mutational history of the SARS-2 lineage  
174 of betacoronaviruses and their metagenomes using the published genomic sequences, despite the  
175 possibilities, in this metagenomic age, of the sort of problems outlined by Chan and Zhan (2020).  
176 We have shown that the 5' third of their genome is largely free of recombinant regions, n-rec,  
177 whereas the remainder is a mélange of recombinant regions from various 'parental' genomes. The  
178 SARS-2 crown group share a distinctive pair of recombinant regions that are most closely related  
179 to the homologous region of the SARS-1 lineage bat virus, Rf4092. A phylogeny calculated from  
180 the 5' n-rec region of the eleven concats shows that the SARS-2 lineage has basal branches of  
181 viruses isolated from pangolins, and a crown group consisting of SARS-2 together with YN02,  
182 RatG13, ZXC21 and ZC45 all of which come from bats, and in that phylogeny SARS-2 is more  
183 closely related to YN02 than RaTG13. This is confirmed by the DnDscan comparisons of the  
184 three viruses. YN02, however, has a recombinant region in its 3' half (nts 21098-24042) of  
185 'unknown' parentage, but which is probably close to the pangolin virus G/1/19, and which is not  
186 present in SARS-2 or RaTG13. Thus, most of the SARS-2 concat, especially its 5' 39%, is closest  
187 to the homologous regions of YN02, but the intact concats of SARS-2 and RaTG13 are more  
188 distant but complete.

189 Our conclusions about the relationships of the SARS-2 crown group are confirmed in the  
190 report of Latinne et al (2020; Fig. 3A) of a large survey of bat viruses of SE Asia. They used  
191 primers to amplify a 440 nts region of the RdRp genes of these viruses, and based their phylogeny  
192 on that region. Although their amplicon overlapped the 3' end of one of the recombinant regions  
193 shared by the SARS-2, YN02 and RaTG13 concats, the overlap is only 78 nts (18%), and the  
194 comparison of the 440 nts amplicons found SARS-2 to be closest to YN02.

195 DnDscan, a simple direct comparison of two sequences, found regions of NS change where  
196 other more complex methods (Angeletti et al., 2020) did not, and we overcame possible problems  
197 with sliding windows (Schmid and Yang, 2008) by making several homologous comparisons. The  
198 NS differences around codon 1000 of the DnDscans are from the DUF3655 region. DUF3655  
199 marks the 5' end of the nsp3 region and is adjacent to its ADP-ribose phosphatase gene (Michalska  
200 et al., 2020). It encodes the N-terminal portion of the nsp3 protein, which has recently been  
201 identified by cryo-electron microscopy as forming hexameric molecular pores spanning the double  
202 membrane of the coronavirus replication organelle (Wolff et al., 2020). The pores probably allow  
203 the progeny SARS-2 genomes to pass from the replication organelle into the lumen of the cytosol,  
204 where their 'structural genes' are translated, and together they are assembled to form progeny  
205 virions (Hsin et al., 2018). Table 2 shows the DUF3655 peptides of the eleven betacoronaviruses  
206 with the acidic and basic residues outlined with different colours; acidic residues in red, and the  
207 few basic residues in blue, and with the theoretical pI of these peptides ranging from 3.01 - 3.40,  
208 in sharp contrast to the nucleocapsid protein encoded by ORF9 which binds the progeny genomes  
209 in the cytosol and has a pI of 10.07 (McBride et al., 2014; Verheije et al., 2010). Table 2 also  
210 shows the secondary structures of the SARS-2 crown group DUF3655 proteins predicted by the  
211 PSIPRED Workbench (Buchan and Jones, 2019). The DUF3655 proteins are found to have similar  
212 N-terminal regions of unstructured residues attached to homologous helical regions, and with C-  
213 termini that are more variable in length and composition. The fact that the DUF3655 protein is so  
214 acidic indicates its likely function in the pore where it may both electrostatically stabilize the lumen  
215 of the pore (Desikan et al., 2020) and ensure that long negatively charged nucleic acid molecules,  
216 like progeny viral genomes, are held centrally in the lumen of the pore as they pass through.

217 The FFPred Prediction database of PSIPRED (Cozzetto et al., 2016) found that the most  
218 likely "biological process" of SARS-2, YN02 and RaTG13 that involves their DUF3655 proteins  
219 is "regulation of metabolic process" (mean probability 0.978) and "regulation of gene expression"  
220 (0.908), their "molecular function" is "nucleic acid binding" (0.966) and "DNA binding" (0.890)  
221 and their "cellular compartment" is "membrane" (0.785).

222 The DUF3655 region seems to have evaded virological, medical and pharmaceutical  
223 scrutiny so far (e.g. Chen and Zhong, 2020; Wei et al., 2020). We suggest that it is probably  
224 involved in a unique rate-limiting step of the coronavirus replicative cycle, and may make CoV  
225 infections susceptible to drugs, like chloroquine, that increase cellular pH  
226 ([https://www.sciencemediacentre.org/expert-reaction-to-questions-around-potential-treatments-  
for-covid-19/](https://www.sciencemediacentre.org/expert-reaction-to-questions-around-potential-treatments-for-covid-19/) March 18 2020). The detailed analysis of this region, specially from residues 9 to

228 27, which have many negatively charged amino acids (Asp and Glu) (Table 2), and probably the  
229 absence of binding sites for macromolecules (RNA, DNA and proteins), would suggest that this  
230 region might be an excellent target for the development of an effective treatment for  
231 sarbecoviruses.

232 The DUF3655 region warrants more attention especially as repetitive acidic amino acids  
233 are present in similar regions of the genomes of human  $\alpha$ CoV (JX504050, KF514433, MT438700),  
234 MERS- $\beta$ CoV (MN481964), bulbul  $\delta$ CoV (NC\_011547) and infectious bronchitis  $\gamma$ CoV  
235 (NC\_001451).

236

237

## 238 **Legends**

239 **Fig. 1.** Maximum likelihood phylogenies of eleven sarbecoviruses calculated from A) their  
240 complete concat sequences; B) only nts 1-11496 of the concat (i.e. the recombinant-free 5' end);  
241 C) the spike protein genes (nts 21315-25143). Acronyms as in Table 1, human viruses in red, bat  
242 viruses in blue and pangolin viruses in gold. Midpoint root circled. All nodes have 1.0 SH support  
243 except, in Fig. 1A, the three terminal nodes of the SARS-2 lineage (mean 0.89 SH) and, in Fig 1C,  
244 the terminal node of the SARS-1 lineage (0.84 SH).

245 **Fig. 2.** Screenshot of the recombinant map of eleven betacoronaviruses analysed using the RDP  
246 version 4.95 program with, above, a simplified genome map showing the positions (yellow) of the  
247 DUF3655, spike and ORF8 genes. The recombinant segments that are statistically supported by  
248 fewer than five methods and  $e^{-5}$  mean probability have a black circle at their 5' end.

249 **Fig. 3.** DnDscan histograms of five pairs of complete betacoronavirus concats; each bar is the  
250 running sum of five S (blue) and NS (gold) codon scores with, above, a simplified genome map  
251 showing the positions (yellow) of the DUF3655, spike and ORF8 genes.

252



253

**Table 1.** Sarbecovirus genomes compared in this study

<b>Accession Code</b>	<b>Host</b>	<b>Isolate (acronym)</b>	<b>Country</b>
EPI_ISL_410721	Pangolin	Guangdong/1/2019 (G/1/19)	China
EPI_ISL_412977	Bat	RmYN02 (YN02)	China
GQ153543	Bat	HKU3-8 (HKU3-8)	HK
KY417145	Bat	Rf4092 (Rf4092)	China
MG772933	Bat	ZC45 (ZC45)	China
MG772934	Bat	ZXC21 (ZXC21)	China
MN996532	Bat	RaTG13 (RaTG13)	China
MT040333	Pangolin	GX-P4L (GX-P4L)	China
MT040336	Pangolin	GXP5E (GXP5E)	China
NC_004718	human	Tor2 (SARS-CoV) (SARS-1)	Canada
NC_045512	human	Wuhan-Hu-1 (SARS-2)	China

254

255

**Table 2.** Comparison of the DUF3655 region of the eleven betacoronaviruses analysed in this study

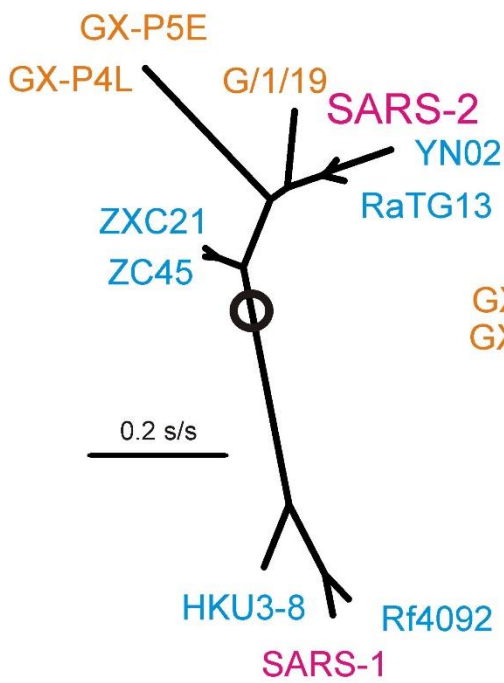
Sequence	pI
SARS-2 MYCSFYPP <b>DEDEEE</b> G <b>CEEEE</b> F <b>EPSTQY</b> -- <b>Y</b> GT <b>EDDYQG</b> <b>K</b> PL <b>FGATS</b> -AAL-QP <b>EEEQ</b> <b>EEDWL</b> <b>DD</b> SQQTVGQQ <b>GS</b> <b>ED</b> <b>NQTTTIQTIV</b> <b>VQPQL</b> <b>EM</b> <b>LTPVVQ</b> - <b>TI</b> <b>E</b> -VN 3.03	
YN02 MYCSFYPP <b>DEDEEE</b> G <b>CEEEE</b> F <b>EPSTQY</b> -- <b>Y</b> GT <b>EDDYR</b> <b>G</b> SL <b>FGATS</b> -AAP-QP <b>EEEQ</b> <b>EEDWL</b> <b>DD</b> ASQQTVAQ <b>E</b> <b>SG</b> <b>NQTT</b> -IQSIV <b>VQPQL</b> <b>EM</b> <b>PTPVVQ</b> - <b>TI</b> <b>E</b> -VN 3.26	
RaTG13 MYCSFYPP <b>DEDEEE</b> G <b>CEEEE</b> F <b>EPPTQY</b> -- <b>Y</b> GT <b>EDDYQG</b> <b>K</b> SL <b>FGATS</b> -VTP-QP <b>EEEL</b> <b>EEDWL</b> <b>DD</b> SQQTVVQ <b>EDS</b> <b>V</b> NQTTITQSI <b>VQPQL</b> <b>EM</b> <b>PTPVVQ</b> -- <b>TI</b> <b>E</b> -VN 3.01	
ZC45 MYCSFYPP- <b>EDE</b> <b>G</b> <b>EDD</b> <b>CE</b> <b>GGQC</b> <b>EPSTQY</b> -- <b>Y</b> GT <b>EDDYQG</b> <b>K</b> PL <b>FGATSFSSS</b> -SQ <b>EEEQ</b> <b>EEDWL</b> <b>ES</b> <b>ISQ</b> <b>E</b> - <b>GQ</b> <b>TAV</b> - <b>N</b> KI <b>----</b> SSV <b>V</b> PPVLQV <b>V</b> STPVVT <b>ETS</b> <b>E</b> -QN 3.31	
ZXC21 MYCSFYPP- <b>EDE</b> <b>G</b> <b>EDD</b> <b>CE</b> <b>GGQF</b> <b>EPSTQY</b> -- <b>Y</b> GT <b>EDDYQG</b> <b>K</b> PL <b>FGATSFSSS</b> -SQ <b>EEEQ</b> <b>EEDWL</b> <b>ES</b> <b>ISQ</b> <b>E</b> - <b>GQ</b> <b>T</b> <b>-----</b> AVT <b>K</b> TS <b>E</b> -QN 3.36	
G/1/19 MYCSFYPP <b>DE</b> Y <b>ED</b> E <b>CE</b> <b>EE</b> <b>QY</b> <b>EPSTQY</b> -- <b>Y</b> GT <b>EDDYQG</b> <b>K</b> SL <b>FGSTS</b> -SAS-QI <b>EEEP</b> <b>EEDWL</b> <b>ED</b> <b>GN</b> <b>EE</b> <b>IAMQ</b> <b>E</b> <b>-----</b> QT <b>----</b> STV <b>V</b> QSQ <b>E</b> <b>I</b> <b>STPVVS</b> <b>E</b> <b>IN</b> <b>SVN</b> 3.08	
GX-P4L MYCSFYPP <b>DE</b> Y <b>ED</b> E <b>YS</b> <b>EE</b> <b>QF</b> <b>EPSTQY</b> -- <b>Y</b> GT <b>ES</b> <b>YK</b> <b>GLPL</b> <b>FGASS</b> -V---QQ <b>EEQ</b> <b>EEDWL</b> <b>ET</b> <b>AV</b> -V <b>EQ</b> <b>V</b> TPT <b>Q</b> <b>EE</b> <b>L</b> <b>----</b> SIT <b>E</b> <b>IVP</b> --AV <b>Q</b> TTIV <b>E</b> <b>----</b> L <b>E</b> - <b>CD</b> 3.11	
GX-P5E MYCSFYPP <b>DE</b> Y <b>ED</b> E <b>YS</b> <b>EE</b> <b>QF</b> <b>EPSTQY</b> -- <b>Y</b> GT <b>ES</b> <b>YK</b> <b>GLPL</b> <b>FGASS</b> -V---QQ <b>EEQ</b> <b>EEDWL</b> <b>ET</b> <b>AV</b> -V <b>EQ</b> <b>V</b> TPT <b>Q</b> <b>EE</b> <b>L</b> <b>----</b> SIT <b>E</b> <b>IVP</b> --AV <b>Q</b> TTIV <b>E</b> <b>----</b> L <b>E</b> - <b>CD</b> 3.11	
HKU3-8 MYCSFYPP <b>DEEED</b> <b>CE</b> <b>CE</b> <b>DEEE</b> <b>IS</b> <b>ET</b> <b>CE</b> <b>Y</b> GT <b>EDDYK</b> <b>GLPL</b> <b>FGAST</b> - <b>T</b> PHV <b>EEEEEEED</b> <b>DW</b> <b>DA</b> <b>IA</b> <b>E</b> <b>----</b> S <b>EP</b> <b>-----</b> <b>E</b> <b>PLP</b> <b>-----</b> <b>EE</b> <b>PVN</b> 3.37	
Rf4092 MYCSFYPP <b>DEEED</b> <b>CE</b> <b>DE</b> <b>DEEE</b> <b>VPE</b> <b>ES</b> <b>CAH</b> <b>Y</b> GT <b>EDDYR</b> <b>GLPL</b> <b>FGAST</b> - <b>E</b> M--QV <b>EEEEEEED</b> <b>WL</b> <b>CA</b> <b>T</b> <b>L</b> - <b>SE</b> <b>H</b> <b>LEP</b> <b>-----</b> <b>E</b> <b>LTP</b> <b>-----</b> <b>EE</b> <b>PVN</b> 3.40	
SARS-1 MYCSFYPP <b>DEEED</b> <b>DA</b> <b>CE</b> <b>EEI</b> <b>DE</b> <b>TC</b> <b>EH</b> <b>Y</b> GT <b>EDDYQ</b> <b>GLPL</b> <b>FGASA</b> - <b>T</b> VR <b>V</b> <b>EEEEEEED</b> <b>DW</b> <b>DT</b> <b>TE</b> <b>Q</b> - <b>SE</b> <b>I</b> <b>EP</b> <b>-----</b> <b>E</b> <b>PTP</b> <b>EE</b> <b>PVN</b> 3.21	

Secondary structure

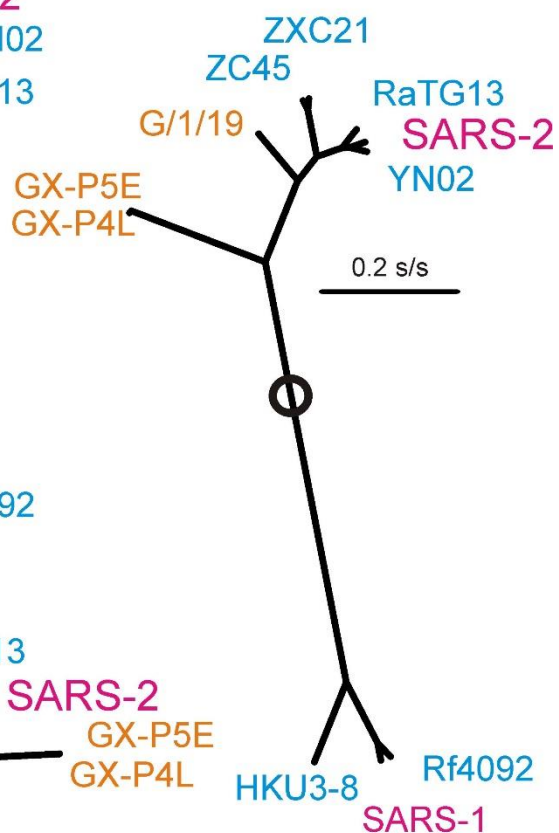
SARS-2	CCCCCCCCCCCCCCCCCCCCCCCCCE--EECCCCCCCCCCCCCCCC--CCC-CCHHHHHCCCCCHHHCCCCCCCCCCCCEEEEEEEEECCCEEEECCEE--EE--CC
YN02	CCCCCCCCCCCCCCCCCCCCCCCCCE--EECCCCCCCCCECCCCCC--CCC-CCHHHHHHHHHHHHHHHHHHHH--CCCCCEE-EEEEEECCCCCCCCCCCE--EE--EC
RaTG13	CCCCCCCCCCCCCCCCCCCCCCCCCE--ECCCCCCCCCEEECCCE--CCC-CCHHHHHHHHCCCCCHCEEECCCCHHHHHHHEEEHHHCCCCCCCCCCCCEE--EE--CC

Fig. 1

A



B



C

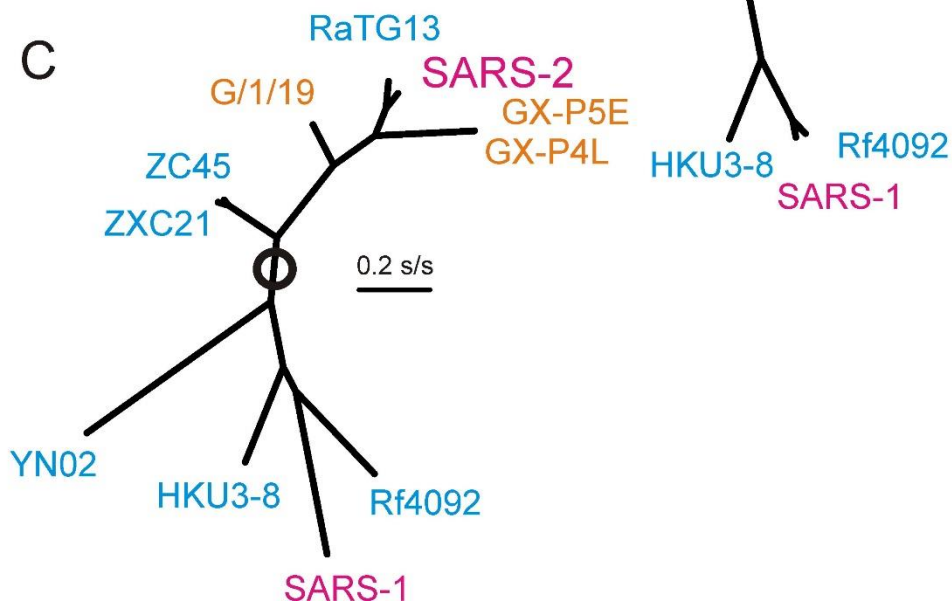


**Fig. 2**

## ORF1ab (nsp1-16)

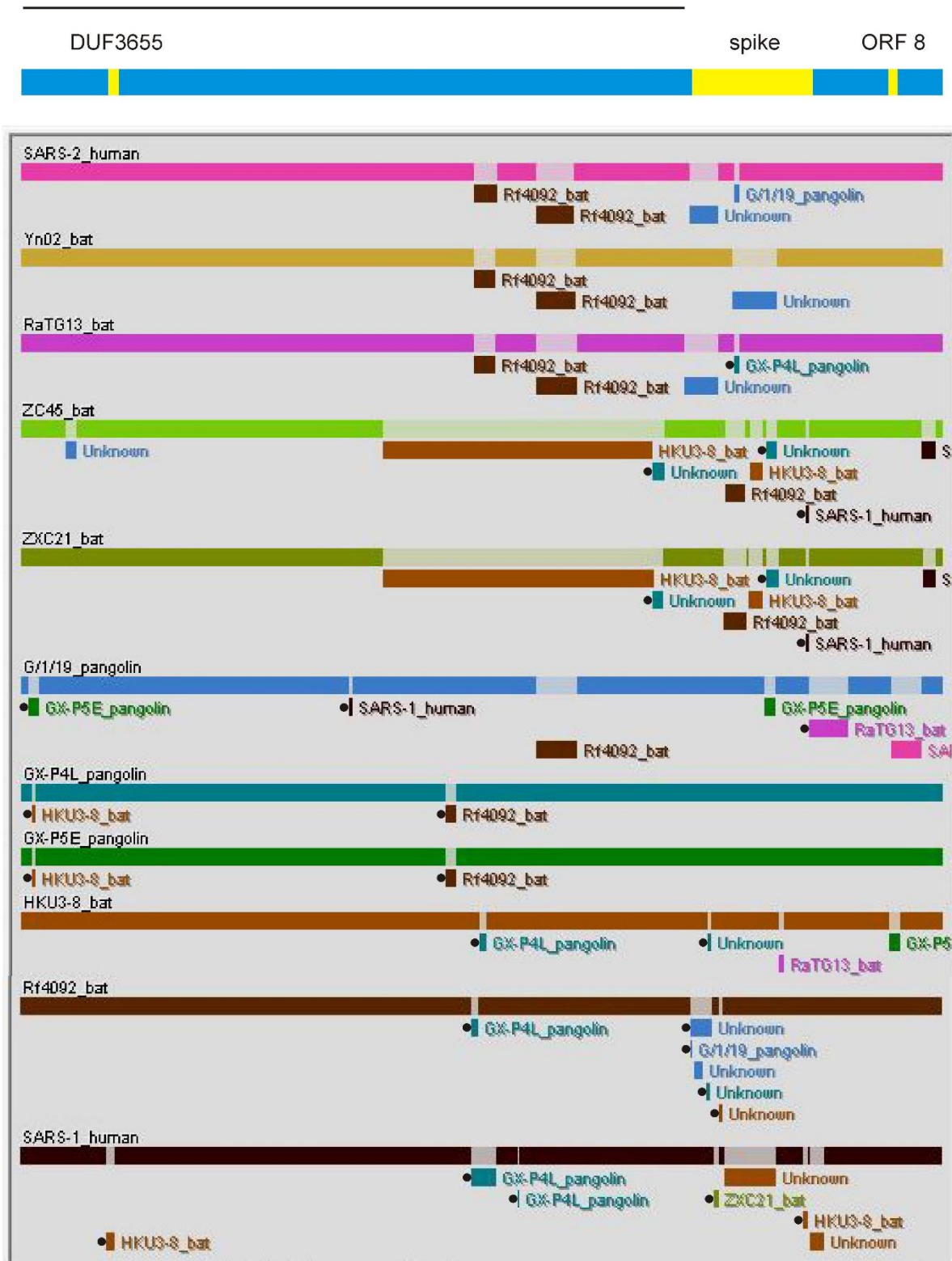
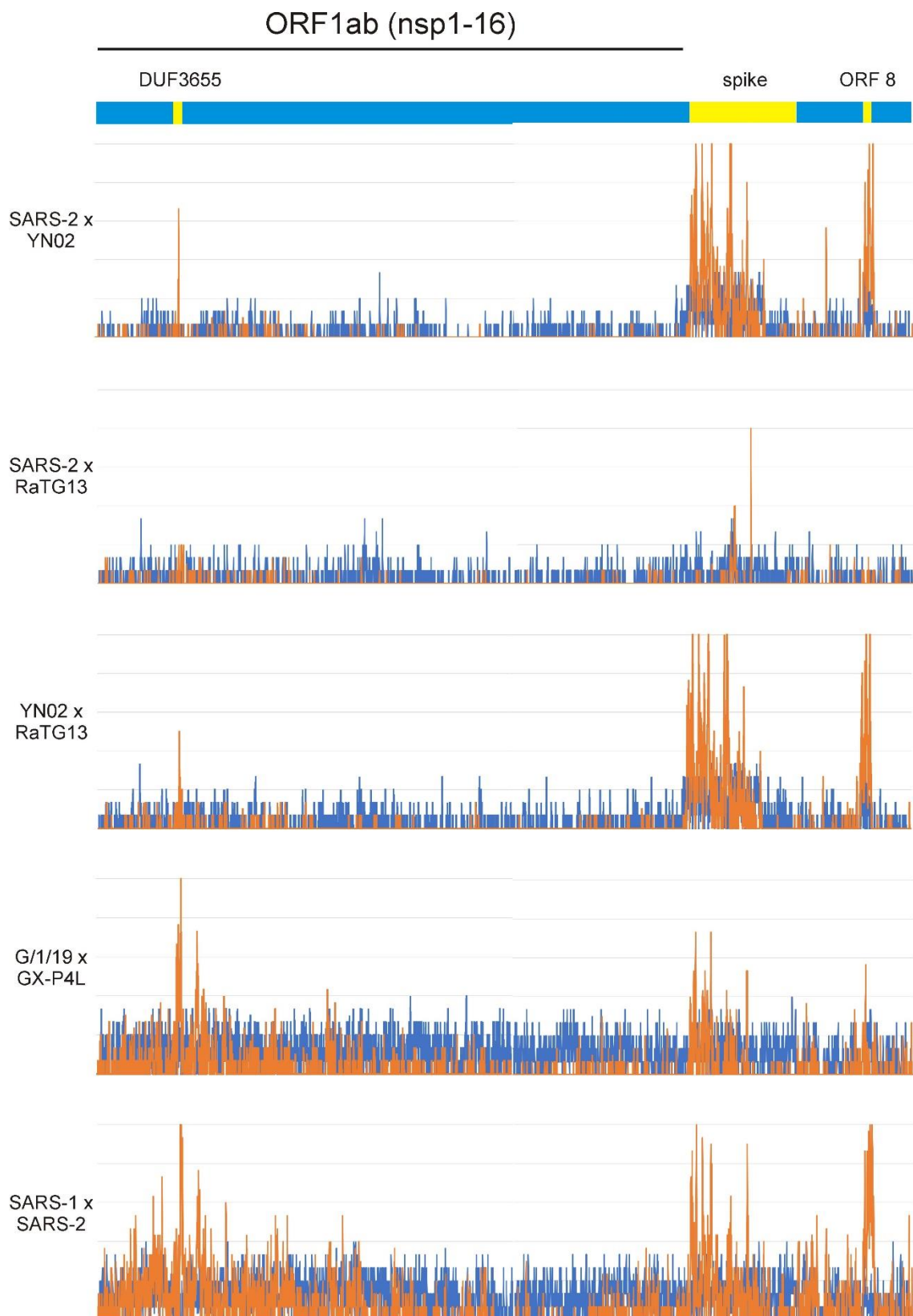


**Fig. 3**





## References

- Abascal, F, Zardoya, R. and Telford, MJ., 2010. TranslatorX: multiple alignment of nucleotide sequences guided by amino acid translations. *Nucleic Acids Res.* 38(2):W7-W13.
- Altschul, SF, et al. 1990. Basic local alignment search tool. *J. Mol. Biol.* 215:403-410.
- Andersen KG, et al. 2020 The proximal origin of SARS-CoV-2. *Nat Med* 26 (4):450-452. doi:10.1038/s41591-020-0820-9
- Angeletti, S. et al. 2020 The role of the nsp2 and nsp3 in its pathogenesis *J Med Virol.* 92:584–588. DOI: 10.1002/jmv.25719
- Anthony SJ, et al Consortium P 2017 Global patterns in coronavirus diversity. *Virus Evol* 3 (1):vex012. doi:10.1093/ve/vex012
- Boni, M. F., Posada, D., & Feldman, M. W. (2007). An exact nonparametric method for inferring mosaic structure in sequence triplets. *Genetics*, 176(2), 1035-1047.
- Buchan DWA, Jones DT 2019 The PSIPRED Protein Analysis Workbench: 20 years on. *Nucleic Acids Research.* <https://doi.org/10.1093/nar/gkz297>
- Candido et al 2020, Evolution and epidemic spread of SARS-CoV-2 in Brazil: <https://www.medrxiv.org/content/10.1101/2020.06.11.20128249>
- Chan, YA. and Zhan, SH. 2020 Single source of pangolin CoVs with a near identical Spike RBD to SARS-CoV-22. bioRxiv preprint doi: <https://doi.org/10.1101/2020.07.07.184374>.
- Chen L, Zhong L, 2020 Genomics functional analysis and drug screening of SARS-CoV-2, *Genes & Diseases*, <https://doi.org/10.1016/j.gendis.2020.04.002>
- Cozzetto D, et al. 2016 FFPred 3: feature-based function prediction for all Gene Ontology domains. *Sci Rep.* 2016 Aug 26;6:31865. doi: 10.1038/srep31865
- Desikan, R. 2020 An In silico Algorithm for Identifying Amino Acids that Stabilize Oligomeric Membrane-Toxin Pores through Electrostatic Interactions bioRxiv preprint doi: <https://doi.org/10.1101/716969>.
- Duchêne et al 2020, Temporal signal and the phylodynamic threshold of SARS-CoV-2. <https://www.biorxiv.org/content/10.1101/2020.05.04.077735v1.full>
- Duchêne S, Holmes EC, Ho SY 2014 Analyses of evolutionary dynamics in viruses are hindered by a time-dependent bias in rate estimates. *Proc Biol Sci* 281, 1786. doi:10.1098/rspb.2014.0732
- Ferron F, et al. 2018 Structural and molecular basis of mismatch correction and ribavirin excision from coronavirus RNA. *Proc Natl Acad Sci U S A.* 115(2):E162-E171. doi: 10.1073/pnas.1718806115. Epub 2017 Dec 26.
- Fourment, M. and Gibbs, M.J., 2006. PATRISTIC: a program for calculating patristic distances and graphically comparing the components of genetic change. *BMC evolutionary biology*, 6(1), 1-5.
- Gasteiger, E. et al 2005. Protein identification and analysis tools on the ExPASy server. In *The proteomics protocols handbook* (pp. 571-607). Humana press.
- Gibbs MJ, et al 2007 The variable codons of H3 influenza A virus haemagglutinin genes. *Arch Virol* 152 (1):11-24. doi:10.1007/s00705-006-0834-8
- Gibbs, MJ., Armstrong, JS., and Gibbs, AJ., 2000. Sister-Scanning: a Monte Carlo procedure for assessing signals in recombinant sequences. *Bioinformatics* 16:573-582.
- Gorbalenya AE, et al Coronaviridae Study Group of the International Committee on Taxonomy of V (2020) The species Severe acute respiratory syndrome-related coronavirus: classifying 2019-nCoV and naming it SARS-CoV-2. *Nature Microbiology* 5 (4):536-544. doi:10.1038/s41564-020-0695-z

- Gribble, J. et al 2020 The coronavirus proofreading exoribonuclease mediates extensive viral recombination bioRxiv preprint doi: <https://doi.org/10.1101/2020.04.23.057786>.
- Guindon, S. and Gascuel, O., 2003. A simple, fast, and accurate algorithm to estimate large phylogenies by maximum likelihood. *Systematic Biol.* 52:696-704.
- Hall, T. A., 1999. BioEdit: a user-friendly biological sequence alignment editor and analysis program for Windows 95/98/NT. *Nucleic Acids Symp. Ser.* 41:95-98.
- Holmes, E. C., Worobey, M., & Rambaut, A. (1999). Phylogenetic evidence for recombination in dengue virus. *Molecular biology and evolution*, 16(3), 405-409.
- Hsin, W. et al 2018 Nucleocapsid protein-dependent assembly of the RNA packaging signal of Middle East respiratory syndrome coronavirus. *J Biomed Sci* 25, 47 (2018). <https://doi.org/10.1186/s12929-018-0449-x>
- Jeanmougin, F. et al 1998. Multiple sequence alignment with Clustal X. *Trends Biochem. Sci.* 23:403-405.
- Katoh, K., and Standley, D. M., 2013. MAFFT multiple sequence alignment software version 7: improvements in performance and usability. *Mol. Biol. Evol.* 30:772-780.
- Latinne, A. et al 2020 Origin and cross-species transmission of bat coronaviruses in China. bioRxiv preprint doi: <https://doi.org/10.1101/2020.05.31.116061>.
- Lemey, P. et al 2009. Identifying recombinants in human and primate immunodeficiency virus sequence alignments using quartet scanning. *BMC Bioinformatics* 10:126.
- Li, X. et al 2020 Emergence of SARS-CoV-2 through Recombination and Strong Purifying Selection Short Title: Recombination and origin of SARS-CoV-2 bioRxiv preprint doi: <https://doi.org/10.1101/2020.03.20.000885.t>
- Lin, X. and Chen, S. 2020 Major Concerns on the Identification of Bat Coronavirus Strain RaTG13 and Quality of Related Nature Paper.Preprints, 2020060044 (doi: 10.20944/preprints202006.0044.v1
- Martin DP et al. 2015 RDP4: Detection and analysis of recombination patterns in virus genomes. *Virus Evol* 1 (1):vev003. doi:10.1093/ve/vev003
- Martin, DP., and Rybicki, E., 2000. RDP: detection of recombination amongst aligned sequences. *Bioinformatics* 16:562-563.
- Martin, DP et al., 2005. A modified bootscan algorithm for automated identification of recombinant sequences and recombination breakpoints. *AIDS Res. Human Retroviruses* 21:98-102.
- Maynard-Smith, J.M., 1992. Analyzing the mosaic structure of genes. *J. Mol. Evol.* 34:126-129.
- McBride R. van Zyl, M. Fielding, BC 2014 Review The Coronavirus Nucleocapsid Is a Multifunctional Protein. *Viruses* 6, 2991-3018; doi:10.3390/v6082991
- McGuire, G., and Wright, F., 2000. TOPAL 2.0: Improved detection of mosaic sequences within multiple alignments. *Bioinformatics* 16:130-134.
- Michalska, K. et al 2020 Crystal structures of SARS-CoV-2 ADP-ribose phosphatase (ADRP): from the apo form to ligand complexes. bioRxiv preprint doi: <https://doi.org/10.1101/2020.05.14.096081>.
- Padidam, M., Sawyer, S., & Fauquet, C. M. (1999). Possible emergence of new geminiviruses by frequent recombination. *Virology*, 265(2), 218-225.
- Posada, D. and Crandall, K. A., 2001. Evaluation of methods for detecting recombination from DNA sequences: computer simulations. *PNAS* 98:13757-13762.

- Prates ET, et al., 2020 Functional Immune Deficiency Syndrome via Intestinal Infection in COVID-19. bioRxiv Confronting the COVID-19 Pandemic with Systems Biology bioRxiv preprint doi: <https://doi.org/10.1101/2020.04.06.028712>. t,
- Pybus, OG et al 2020, Preliminary analysis of SARS-CoV-2 importation & establishment of UK transmission lineages: "E " (<https://virological.org/t/preliminary-analysis-of-sars-cov-2-importation-establishment-of-uk-transmission-lineages/507/2>).
- Resende et al 2020, Genomic surveillance of SARS-CoV-2 reveals community transmission of a major lineage during the early pandemic phase in Brazil: "<https://virological.org/t/genomic-surveillance-of-sars-cov-2-reveals-community-transmission-of-a-major-lineage-during-the-early-pandemic-phase-in-brazil/514>".
- Rodríguez-Román E, Gibbs AJ. Ecology and Evolution of Betacoronaviruses. In: Rezaei N, ed. Coronavirus disease (COVID-19). Springer Nature 2020. In press.
- Schmid K, Yang Z 2008 The trouble with sliding windows and the selective pressure in BRCA1. PLoS ONE 3(11): e3746. doi:10.1371/journal.pone.0003746
- Shimodaira, H., & Hasegawa, M. (1999). Multiple comparisons of log-likelihoods with applications to phylogenetic inference. *Molecular biology and evolution*, 16(8), 1114-1114.
- Verheije, MH 2010 The Coronavirus Nucleocapsid Protein Is Dynamically Associated with the Replication-Transcription Complexes *J. Virol.* 84. 11575–11579
- Wang, H., Pipes, L. Nielsen, R. (2020) Synonymous mutations and the molecular evolution of SARS-Cov-2 origins bioRxiv preprint doi: <https://doi.org/10.1101/2020.04.20.052019>
- Wei, J. et al. 2020 Genome-wide CRISPR screen reveals host genes that regulate SARS-CoV-2 infection bioRxiv preprint doi: <https://doi.org/10.1101/2020.06.16.155101>.
- Wolff, G. 2020 A molecular pore spans the double membrane of the coronavirus replication organelle bioRxiv preprint doi: <https://doi.org/10.1101/2020.06.25.171686>.
- Wu, F., Zhao, S., Yu, B. et al. A new coronavirus associated with human respiratory disease in China. *Nature* 579, 265–269 (2020). <https://doi.org/10.1038/s41586-020-2008>
- Xiao, K. et al. 2020 Isolation of SARS-CoV-2-related coronavirus from Malayan pangolins. *Nature* (2020) doi:10.1038/s41586-020-2313-x.
- Ye, W. et al 2020 Zoonotic origins of human coronaviruses *Int. J. Biol. Sci.* 16(10): 1686-1697. doi: 10.7150/ijbs.45472
- Zhou P et al. 2020 A pneumonia outbreak associated with a new coronavirus of probable bat origin. *Nature* 579 (7798):270-273. doi:10.1038/s41586-020-2012-7